Sequential breakdown of 3-phosphorylated phosphoinositides is essential for the completion of macropinocytosis

Masashi Maekawa[a,b,1], Shimpei Terasaka[a,1], Yasuhiro Mochizuki[c], Katsuhisa Kawai[d], Yuka Ikeda[d], Nobukazu Araki[d], Edward Y. Skolnik[e], Tomohiko Taguchi[a,f,2], and Hiroyuki Arai[a,f,2]

[a]Department of Health Chemistry and [f]Pathological Cell Biology Laboratory, Graduate School of Pharmaceutical Sciences, University of Tokyo, Tokyo 113-0033, Japan; [c]Department of Molecular Biology and Medicine, Research Center for Advanced Science and Technology, University of Tokyo, Tokyo 153-8904, Japan; [d]Department of Histology and Cell Biology, School of Medicine, Kagawa University, Miki, Kagawa 761-0793, Japan; [e]Division of Nephrology, Department of Pharmacology, The Helen L. and Martin S. Kimmel Center for Biology and Medicine at the Skirball Institute for Biomolecular Medicine, New York University Langone Medical Center, New York, NY 10016; and [b]Keenan Research Centre, Li Ka Shing Knowledge Institute, St. Michael's Hospital, Toronto, ON, Canada M5B1W8

Edited by Pietro De Camilli, Yale University and Howard Hughes Medical Institute, New Haven, CT, and approved February 3, 2014 (received for review June 12, 2013)

Macropinocytosis is a highly conserved endocytic process by which extracellular fluid and solutes are internalized into cells. Macropinocytosis starts with the formation of membrane ruffles at the plasma membrane and ends with their closure. The transient and sequential emergence of phosphoinositides PI(3,4,5)P_3 and PI(3,4)P_2 in the membrane ruffles is essential for macropinocytosis. By making use of information in the *Caenorhabditis elegans* mutants defective in fluid-phase endocytosis, we found that mammalian phosphoinositide phosphatase MTMR6 that dephosphorylates PI(3)P to PI, and its binding partner MTMR9, are required for macropinocytosis. INPP4B, which dephosphorylates PI(3,4)P_2 to PI(3)P, was also found to be essential for macropinocytosis. These phosphatases operate after the formation of membrane ruffles to complete macropinocytosis. Finally, we showed that KCa3.1, a Ca^{2+}-activated K^+ channel that is activated by PI(3)P, is required for macropinocytosis. We propose that the sequential breakdown of PI(3,4,5)P_3 → PI(3,4)P_2 → PI(3)P → PI controls macropinocytosis through specific effectors of the intermediate phosphoinositides.

Endocytosis is the uptake of membrane proteins, lipids, extracellular ligands, solutes, and particles from the plasma membrane (PM) into the intracellular milieu (the cytoplasm) by membrane-bound vesicles. Endocytosis occurs by multiple mechanisms that fall into two broad categories: "pinocytosis" (the uptake of fluid and solutes) and "phagocytosis" (the uptake of large particles) (1). Pinocytosis occurs in virtually all cells, whereas phagocytosis is typically restricted to specialized mammalian cells. Macropinocytosis differs from other known pinocytic pathways, such as the clathrin-mediated and lipid raft-mediated pathways, in that it is preceded by vigorous PM activity in the form of actin-rich membrane ruffling (2, 3). Membrane ruffles turn into circular ruffles, then circular ruffles fuse or close, resulting in massive internalization of extracellular fluid and solutes into vacuoles (0.2–10 μm), called macropinosomes, which are larger than other pinocytic vesicles (2). Their formation often results in a transient increase in cellular fluid uptake (10-fold over baseline) (4, 5). In most cell types, macropinocytosis is a transient process (4–6). Physiological ligands, such as growth factors and integrin substrates, serve as specific triggers (4, 7, 8). In immune responses, dendritic cells use macropinocytosis to take up extracellular antigens, leading to their presentation on class I and class II major histocompatibility complex molecules (9, 10). Some bacteria and viruses also take advantage of macropinocytosis to invade host cells by activating growth factor receptors or other signaling molecules (11). Ras-transformed tumor cells use macropinocytosis to take up extracellular proteins to support their unique metabolic needs (12).

Phosphoinositides, phosphorylated inositol lipids, are involved in many cellular processes, such as signal transduction and membrane dynamics (13–15). Macropinocytosis seems to be regulated by several phosphoinositides. Inhibitors of phosphoinositide 3-kinases (PI3Ks), which generate PI(3,4,5)P_3 from PI(4,5)P_2, impair macropinosome formation (16). Knockdown of 5-phosphatase SH2-domain containing inositol-5-phosphatase 2 (SHIP2), which dephosphorylates PI(3,4,5)P_3 to PI(3,4)P_2, suppresses macropinocytic uptake of extracellular solutes (17). The dynamic nature of phosphoinositides during macropinocytosis has been described. In EGF-stimulated A431 cells, the PI(4,5)P_2 level increases in membrane ruffles, reaches its maximum before circular ruffle formation, and rapidly falls afterward (18). In contrast, the PI(3,4,5)P_3 level increases in circular ruffles and peaks at the beginning of circular ruffle fusion. In macrophage colony-stimulating factor–stimulated macrophages, transient and sequential spikes of PI(4,5)P_2, PI(3,4,5)P_3, PI(3,4)P_2, and PI(3)P in membrane ruffles are observed during macropinocytosis (19, 20). These studies also suggest the presence of a diffusion barrier that restricts the phosphoinositides within membrane ruffles. The presence of a diffusion

Significance

Macropinocytosis is a form of endocytosis that is accompanied by ruffling of plasma membrane and participates in a diverse range of pathophysiological processes, such as antigen uptake by immune cells and tumor growth. However, the molecular mechanism underlying this process is poorly understood. By exploiting the studies of fluid-phase endocytosis in *Caenorhabditis elegans*, we found that dephosphorylation of phosphoinositide PI(3)P is essential for macropinocytosis in mammalian cells. We also found that the sequential dephosphorylation of PI(3,4,5)P_3 → PI(3,4)P_2 → PI(3)P → PI at membrane ruffles is required for macropinocytosis. Identification of phosphoinositide phosphatases in the dephosphorylation cascade and a PI(3)P-sensitive K^+ channel as essential factors for macropinocytosis may provide the way to selectively control macropinocytosis among various endocytic pathways.

Author contributions: M.M., S.T., E.Y.S., T.T., and H.A. designed research; M.M., S.T., K.K., Y.I., and N.A. performed research; Y.M. and E.Y.S. contributed new reagents/analytic tools; M.M., S.T., K.K., Y.I., N.A., and T.T. analyzed data; and T.T. and H.A. wrote the paper.

The authors declare no conflict of interest.

This article is a PNAS Direct Submission.

Freely available online through the PNAS open access option.

[1]M.M. and S.T. contributed equally to this work.

[2]To whom correspondence may be addressed. E-mail: tom_taguchi@mol.f.u-tokyo.ac.jp or harai@mol.f.u-tokyo.ac.jp.

This article contains supporting information online at www.pnas.org/lookup/suppl/doi:10.1073/pnas.1311029111/-/DCSupplemental.

barrier was also supported by the study using membrane-tethered photoactivatable green fluorescent protein (21).

In *Caenorhabditis elegans*, an in vivo assay for fluid-phase endocytosis has been developed using coelomocytes, which are scavenger cells that endocytose fluid from the body cavity (22, 23). The assay uses transgenic worms in which GFP tagged with a secretory signal sequence (*myo-3p::ssGFP*) is secreted into the body cavity from body wall muscle cells (Fig. S1*A*). The GFP is endocytosed primarily by coelomocytes and is subsequently degraded. In CUP (coelomocyte uptake defective) mutants, GFP is not endocytosed by coelomocytes and therefore accumulates in the body cavity. Genes whose mutations impair fluid-phase endocytosis in coelomocytes are defined as CUP genes (Table S1). Among the CUP genes, *mtm-6* and *mtm-9* encode phosphoinositide 3-phosphatases that belong to the myotubularin family (24, 25). In the present study we found that the mammalian orthologs [myotubularin-related protein 6 (MTMR6) and myotubularin-related protein 9 (MTMR9)] of *mtm-6* and *mtm-9* are required for macropinocytosis through dephosphorylation of PI(3)P to PI. We then found that INPP4B, which dephosphorylates PI(3,4)P_2 to PI(3)P, is also required for macropinocytosis. It has been reported that SHIP2, which dephosphorylates PI(3,4,5)P_3 to PI(3,4)P_2, is required for macropinocytosis (17). Together, these findings suggest that macropinocytosis is controlled by the sequential breakdown of PI(3,4,5)P_3 → PI(3,4)P_2 → PI(3)P → PI in the PM. Furthermore, we showed that KCa3.1, a Ca^{2+}-activated K^+ channel that is activated by a PI(3)P (26–28), is essential for macropinocytosis.

Results

MTM-6 and MTM-9 Function Cell-Autonomously in Fluid-Phase Endocytosis in Coelomocytes. As reported previously (29), *mtm-6* and *mtm-9* mutants revealed a severe CUP phenotype, with the accumulation of GFP in the body cavity and no GFP in coelomocytes (Fig. S1*B*). To investigate the cell autonomy of the defect in coelomocytes, we performed an ex vivo fluid-phase endocytosis assay (30) with isolated coelomocytes from transgenic worms (31), in which α-mannosidase II-GFP (MANS-GFP) is expressed specifically in coelomocytes. As shown in Fig. 1 *A* and *B*, coelomocytes isolated from WT worms endocytosed a fluid-phase marker, tetramethylrhodamine (TMR)-conjugated dextran, whereas coelomocytes isolated from *mtm-6* and *mtm-9* mutants did not. These data show that MTM-6 and MTM-9 function cell-autonomously in fluid-phase endocytosis in coelomocytes.

MTMR6 and MTMR9 Are Essential for Macropinocytosis in A431 Cells. We asked whether mammalian orthologs (MTMR6 and MTMR9) of *mtm-6* and *mtm-9* are required for macropinocytosis, a fluid-phase endocytosis in mammalian cells. MTMR6 is a phosphoinositide 3-phosphatase. MTMR9 increases the enzyme activity and the stability of MTMR6 by forming a heterodimer with MTMR6 (32). A431 human epidermoid carcinoma cells show a rapid (within 30 s to 1 min) but transient macropinocytic activity (5–10 min) after EGF stimulation. As previously reported (4, 5, 33), serum-starved A431 cells increased the uptake of TMR-dextran in an EGF-dependent manner (Fig. S2*A*). The increase in fluid-phase uptake by EGF stimulation was significantly suppressed by pretreatment of cells with amiloride, an inhibitor of macropinocytosis (5, 34). The EGF-dependent, amiloride-sensitive uptake of dextran in A431 cells was quantitatively confirmed by FACS analysis (Fig. S2*B*). Knockdown of either MTMR6 or MTMR9, like knockdown of PAK-1 (p21-activated kinase-1), an essential factor for macropinocytosis (35–37), significantly inhibited the dextran uptake (Fig. 2 *A* and *B*). Knockdown with other siRNAs for MTMR6 or MTMR9 revealed a correlation between the knockdown efficiency and the degree of inhibition of macropinocytosis (Fig. S2*C*). The knockdown of MTMR6 or MTMR9 did not impair the uptake of transferrin (Tfn) from the PM (Fig. S3), which is dependent on clathrin (38). These findings show the specificity of MTMR6 and MTMR9 in endocytic pathways: MTMR6 and MTMR9 are essential for macropinocytosis but not for clathrin-dependent endocytosis.

We then asked whether the phosphoinositide 3-phosphatase activity of MTMR6 (39) is required for macropinocytosis. The catalytic activity of myotubularin family proteins is mediated by an active site sequence "CX_5R" present in the protein tyrosine phosphatase (PTP) domain (24, 40) (Fig. S4). Cells were depleted of MTMR6 with siRNA#2 and transfected with an siRNA-resistant MTMR6 construct (mouse WT or mouse CR/AA mutant in which the CX_5R motif is mutated). The expression of mouse WT in MTMR6-depleted cells restored dextran uptake, comparable to cells treated with control siRNA (Fig. 2*C* and Fig. S4). In contrast, the expression of mouse CR/AA mutant did not rescue the defect of the dextran uptake. Therefore, the enzymatic activity of MTMR6 is essential for macropinocytosis.

MTMR6 and MTMR9 Are Not Required for Membrane Ruffle Formation. We sought to elucidate in which step(s) MTMR6 and MTMR9 function in macropinocytosis. Macropinocytosis begins with membrane-ruffle formation (2, 5). Ruffles are actin-rich, sheet-like extensions of PM, distributed over the dorsal surfaces of cells (6, 16). Some ruffles turn into circular ruffles, then subsequently close or fuse, resulting in the formation of intracellular macropinosomes (19, 33). We found, by phalloidin staining of F-actin and scanning EM, that cells depleted of MTMR6 or MTMR9 still induced actin polymerization (Fig. 2*D*) and formed membrane ruffles after EGF stimulation (Fig. 2*E*). In contrast, in cells depleted of PAK-1, little F-actin staining was observed after EGF stimulation (Fig. 2*D*).

Macropinosome formation was monitored by live cell imaging. As reported (18, 33), time-lapse video microscopy of A431 cells stimulated with EGF revealed that prominent phase-dark ruffles originated from the cell periphery and moved along the dorsal cell surface toward the center of the cells (Movie S1). During this process, some ruffles subsequently close, resulting in the formation of phase-bright macropinosomes (Fig. 2*F*, arrowheads). In cells depleted of MTMR6 or MTMR9, the formation of phase-dark ruffles and their movement were active like control cells, but the formation of macropinosomes was severely impaired (Fig. 2*F* and Movies S2 and S3). These data clearly showed that MTMR6 and MTMR9 function in the steps that follow the formation of membrane ruffles, toward the completion of macropinocytosis.

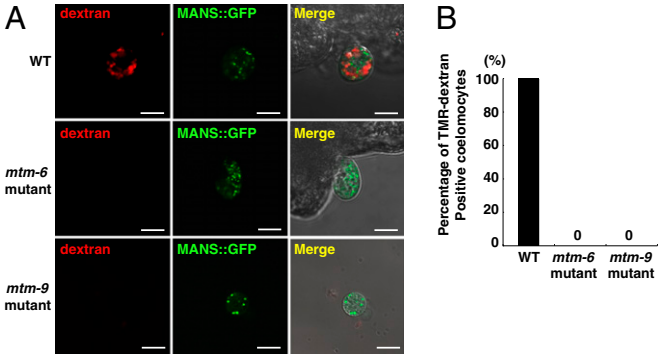

Fig. 1. Cell-autonomous function of MTM-6 and MTM-9 in fluid-phase endocytosis in coelomocytes. (*A*) Confocal images of isolated coelomocytes incubated with TMR-dextran (70,000 MW) in CO_2 independent medium for 20 min. All worms contain the *pcc-1::MANS::GFP* array, which is expressed specifically in coelomocytes. (Scale bars, 10 μm.) (*B*) Percentage of TMR-dextran–positive coelomocytes in ex vivo uptake assay. $n = 10$.

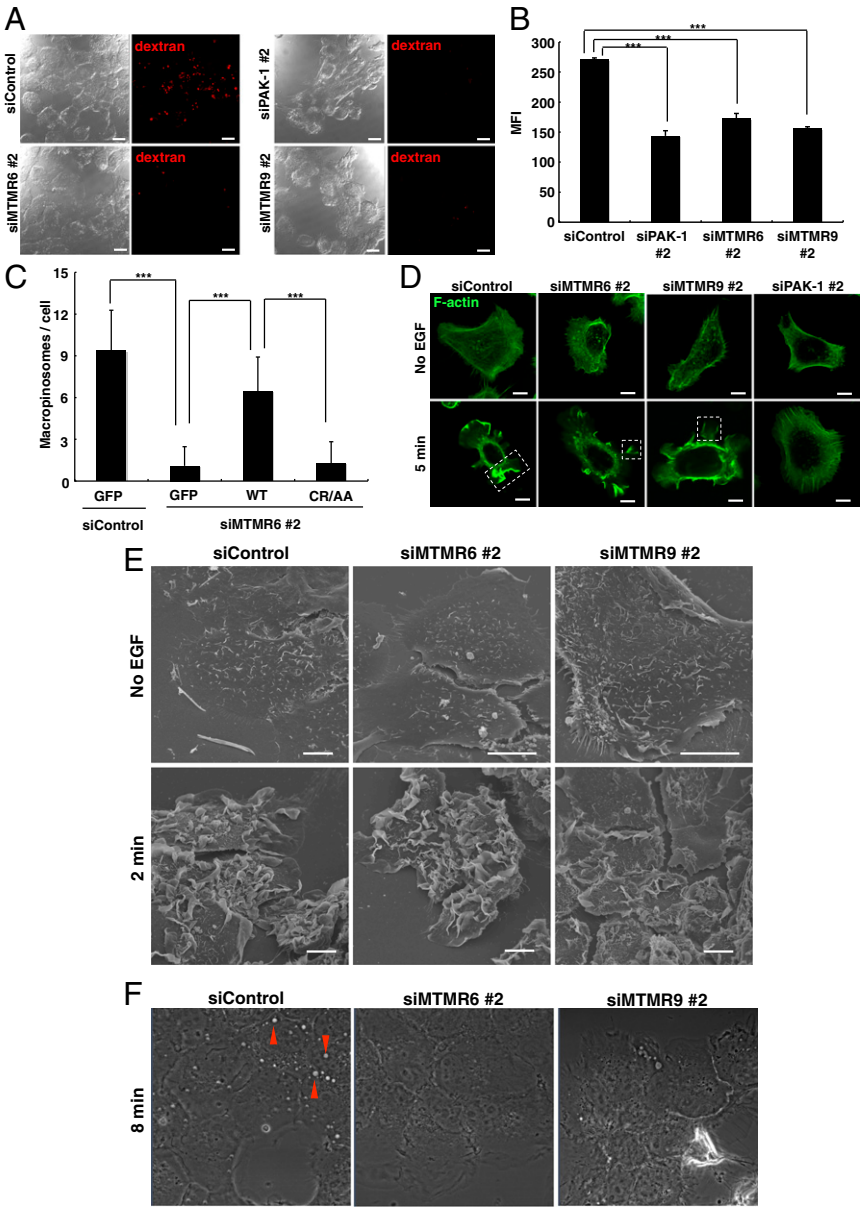

Fig. 2. MTMR6 and MTMR9 are essential for macropinocytosis. (*A*) Cells were treated with the indicated siRNAs and then stimulated by EGF for the uptake of TMR-dextran for 5 min. Brightfield and TMR-dextran fluorescence images are shown. (Scale bars, 20 μm.) (*B*) Cells processed as in *A* with fluorescein-dextran were subjected to FACS analysis. Data represent mean fluorescence intensity (MFI) ± SEM (n = 3). ***P < 0.001. (*C*) Cells were either treated with control siRNA or MTMR6 siRNA, then transfected with the indicated plasmids. The number of macropinosomes positive with TMR-dextran 5 min after EGF stimulation is counted. Data represent mean ± SEM (n = 12). ***P < 0.001. (*D*) F-actin staining by phalloidin in cells depleted of MTMR6, MTMR9, or PAK-1 with or without EGF stimulation. Representative F-actin–positive ruffles are indicated by rectangles. (Scale bars, 10 μm.) (*E*) Scanning electron micrographs of cells depleted of MTMR6 or MTMR9 with or without EGF stimulation. (Scale bars, 10 μm.) (*F*) Phase-contrast images 8 min after EGF stimulation of cells treated with the indicated siRNAs. Representative macropinosomes (phase-bright objects) are indicated by red arrowheads. Note that macropinosomes were formed only in control cells after EGF stimulation.

MTMR6 and MTMR9 Are Recruited to Membrane Ruffles upon EGF Stimulation. We next determined the intracellular localizations of MTMR6 and MTMR9 during macropinocytosis. In nonstimulated A431 cells, myc-MTMR6 and myc-MTMR9 showed a diffusive pattern throughout the cytoplasm, which did not colocalize with calnexin, an ER protein (Fig. 3*A*). This indicates that MTMR6 and MTMR9 localize mostly in the cytosol, as is the case of MDCK cells (41). In contrast, 5 min after EGF stimulation, MTMR6 and MTMR9 were found in membrane ruffles at the cell periphery (Fig. 3*A*), which were enriched in F-actin (Fig. 3*B*). MTMR6 or MTMR9 was expressed together with mCherry, and cells were stimulated for 5 min with EGF (Fig. S5). Fluorescence intensity profile clearly showed the enrichment of MTMR6 and MTMR9 over cytosolic mCherry at membrane ruffles. Therefore, MTMR6 and MTMR9 relocated to the PM, specifically to membrane ruffles after EGF stimulation.

We then asked which domains of MTMR6/MTMR9 mediate membrane targeting. Four constructs [pleckstrin homology–glucosyltransferases, rab-like GTPase activators and myotubularins (PHG) domain of MTMR6, PHG domain of MTMR9, MTMR6 that lacks PHG domain, and MTMR9 that lacks PHG domain] were constructed and expressed in cells. The former two were targeted to membrane ruffles 5 min after EGF stimulation, whereas the latter two were not (Fig. 3*C*), indicating that the PHG domains are necessary and sufficient for targeting of MTMR6/MTMR9 to membrane ruffles.

INPP4B, 4-Phosphatase of PI(3,4)P_2, Is Essential for Macropinocytosis. Recent studies have shown that PI(3,4,5)P_3 and PI(3,4)P_2 are transiently generated in membrane ruffles and dissipated during macropinocytosis (17–20). Moreover, PI3K and 5-phosphatase SHIP2 have been shown to be required for macropinocytosis through phosphorylation of PI(4,5)P_2 and dephosphorylation of PI(3,4,5)P_3, respectively (Fig. 4*A*) (16, 17). Given that MTMR6 is a 3-phosphatase (39), we speculated that PI(3,4)P_2 is dephosphorylated by 4-phosphatase to provide the substrate PI(3)P to MTMR6. To date, inositol polyphosphate 4-phosphatase type I (INPP4A) and inositol polyphosphate 4-phosphatase type II (INPP4B) are known as specific 4-phosphatases of PI(3,4)P_2, leading to the generation of PI(3)P (42–44). Because we detected

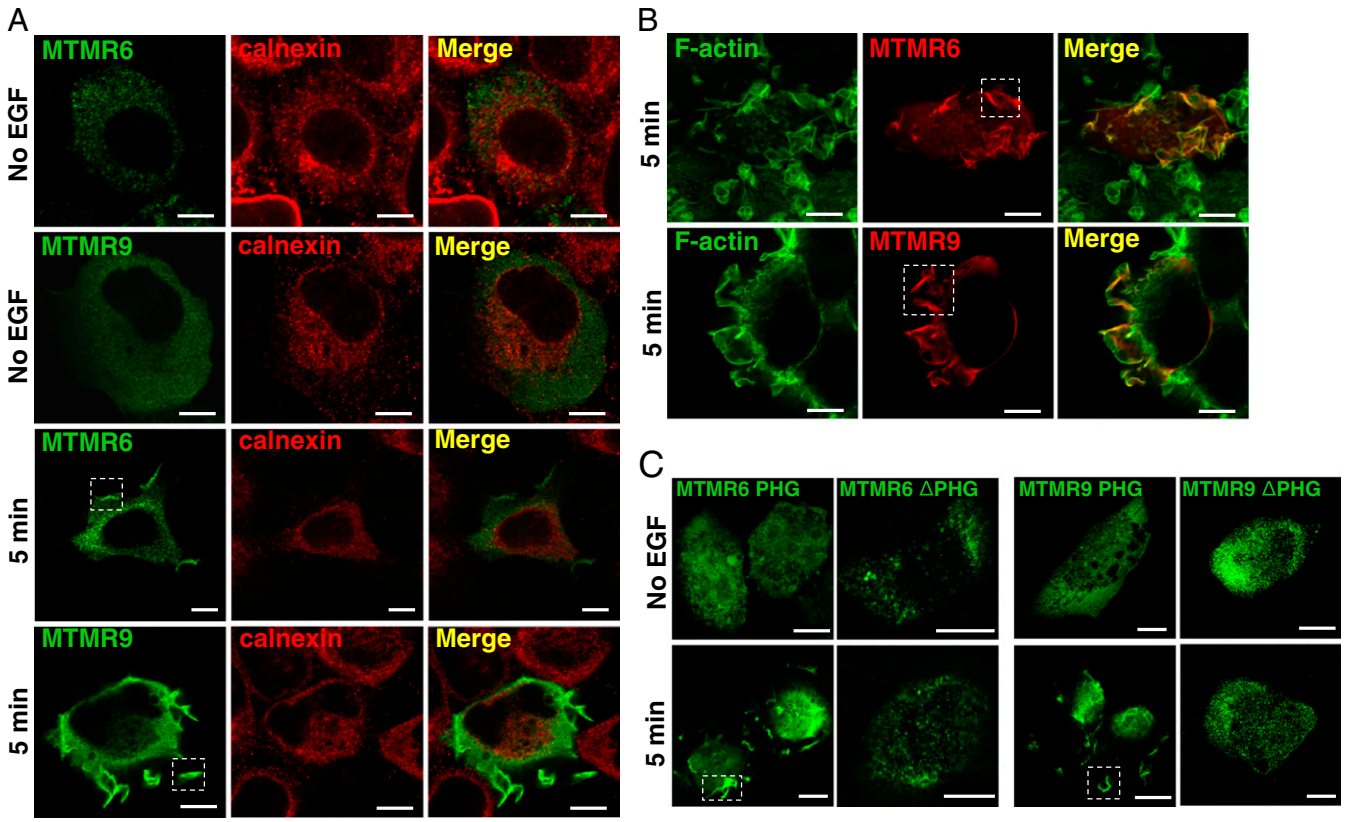

Fig. 3. Effects of EGF stimulation on MTMR6 and MTMR9 localization. (*A*) Cells were transfected with myc-mouse MTMR6 or myc-mouse MTMR9. Cells with or without EGF stimulation were fixed, permeabilized, and coimmunostained for myc and calnexin. MTMR6 and MTMR9 in membrane ruffles after EGF stimulation are indicated by rectangles. (*B*) Cells were transfected with myc-mouse MTMR6 or myc-mouse MTMR9. Cells were fixed 5 min after EGF stimulation, permeabilized, and costained for myc and F-actin with phalloidin. MTMR6 and MTMR9 in membrane ruffles after EGF stimulation are indicated by rectangles. (*C*) Cells were transfected with GFP-MTMR6 PHG, myc-MTMR6 ΔPHG, GFP-MTMR9 PHG, or myc-MTMR9 ΔPHG. Cells with or without EGF stimulation were fixed, permeabilized, and immunostained for myc when necessary. MTMR6 PHG and MTMR9 PHG in membrane ruffles after EGF stimulation are indicated by rectangles. (Scale bars in *A*–*C*, 10 μm.)

the expression of INPP4B mRNA but not that of INPP4A mRNA in A431 cells, we focused on INPP4B for the subsequent experiments.

In cells depleted of INPP4B with siRNA#1, as in cells depleted of PAK-1, MTMR6, or MTMR9, the uptake of dextran was significantly impaired (Fig. 4 *B* and *C*). Knockdown with other siRNAs for INPP4B revealed a correlation between the knockdown efficiency and the degree of inhibition of macropinocytosis (Fig. S6*A*). Clathrin-dependent Tfn uptake was not impaired by INPP4B knockdown (Fig. S6 *B* and *C*). Like knockdown of MTMR6 and MTMR9, knockdown of INPP4B did not inhibit EGF-stimulated membrane ruffle formation (Fig. 4*D*) or actin polymerization (Fig. 4*E*). Live imaging showed that the formation of macropinosomes, but not the formation of phase-dark ruffles and their movement, was severely impaired in cells depleted of INPP4B (Fig. 4*F* and Movies S4 and S5). Thus, like MTMR6 and MTMR9, INPP4B functions in the steps that follow the formation of membrane ruffles.

Dynamics of Phosphoinositides in Membrane Ruffles During Macropinocytosis. We thus found that 3-phosphatase MTMR6/MTMR9 and 4-phosphatase INPP4B are required for macropinocytosis. It has been reported that 5-phosphatase SHIP2 is required for macropinocytosis (17). These findings suggest that $PI(3,4,5)P_3$ is sequentially dephosphorylated to PI by these phosphatases in membrane ruffles. To test this idea, GFP-tagged probes specific for phosphoinositides were expressed, and their dynamics were examined.

$PI(3,4,5)P_3$, which was probed by Akt1-PH (45), appeared in membrane ruffles 3 min after EGF stimulation and dissipated mostly by 10 min in control cells (Fig. 5*A*), as reported previously (18). In contrast, $PI(3,4,5)P_3$ lingered in membrane ruffles even 10 min after EGF stimulation in cells depleted of SHIP2, indicating that SHIP2 mediates $PI(3,4,5)P_3$ dephosphorylation in membrane ruffles. Knockdown of INPP4B or MTMR6 did not influence the dynamics of $PI(3,4,5)P_3$ (Fig. S7*B*).

$PI(3,4)P_2$, which was probed by TAPP1-PH (46), appeared in membrane ruffles after EGF stimulation and dissipated mostly 10 min after EGF stimulation in control cells (Fig. 5*B*). The transient appearance of $PI(3,4)P_2$ is in good accordance with the previous observations in different cell lines (17, 20). In contrast, $PI(3,4)P_2$ lingered in membrane ruffles even 10 min after EGF stimulation in cells depleted of INPP4B, indicating that INPP4B mediates $PI(3,4)P_2$ dephosphorylation in membrane ruffles. Knockdown of SHIP2 abolished the appearance of $PI(3,4)P_2$ (Fig. 5*B*), suggesting that $PI(3,4)P_2$ generated in membrane ruffles is derived from $PI(3,4,5)P_3$. Knockdown of MTMR6 did not influence the dynamics of $PI(3,4)P_2$ (Fig. S7*A*).

PI(3)P, which was probed by EEA1-2xFYVE (47), was not detectable in membrane ruffles after EGF stimulation in control cells (Fig. 5*C*). In contrast, in cells depleted of MTMR6, PI(3)P was found in a number of membrane ruffles after EGF stimulation. These results indicate that PI(3)P emerges and then disappears rapidly by dephosphorylation with MTMR6 in EGF-stimulated cells. Double knockdown of MTMR6 and SHIP2 or that of MTMR6 and INPP4B abolished the emergence of PI(3)P after

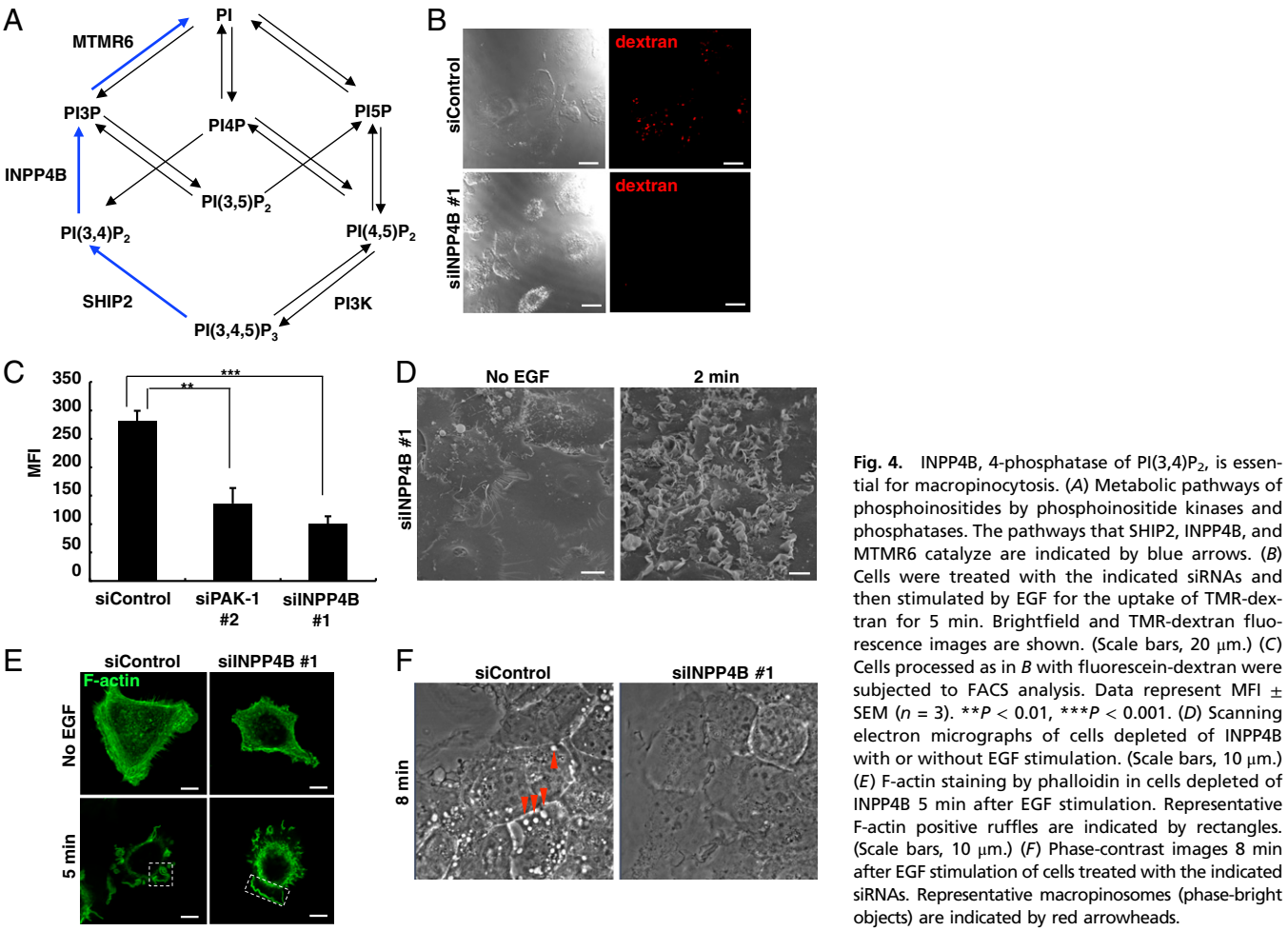

Fig. 4. INPP4B, 4-phosphatase of PI(3,4)P_2, is essential for macropinocytosis. (*A*) Metabolic pathways of phosphoinositides by phosphoinositide kinases and phosphatases. The pathways that SHIP2, INPP4B, and MTMR6 catalyze are indicated by blue arrows. (*B*) Cells were treated with the indicated siRNAs and then stimulated by EGF for the uptake of TMR-dextran for 5 min. Brightfield and TMR-dextran fluorescence images are shown. (Scale bars, 20 μm.) (*C*) Cells processed as in *B* with fluorescein-dextran were subjected to FACS analysis. Data represent MFI ± SEM (n = 3). $^{**}P < 0.01$, $^{***}P < 0.001$. (*D*) Scanning electron micrographs of cells depleted of INPP4B with or without EGF stimulation. (Scale bars, 10 μm.) (*E*) F-actin staining by phalloidin in cells depleted of INPP4B 5 min after EGF stimulation. Representative F-actin positive ruffles are indicated by rectangles. (Scale bars, 10 μm.) (*F*) Phase-contrast images 8 min after EGF stimulation of cells treated with the indicated siRNAs. Representative macropinosomes (phase-bright objects) are indicated by red arrowheads.

EGF stimulation, indicating that PI(3)P in membrane ruffles is derived from PI(3,4,5)P_3 and PI(3,4)P_2. Live cell imaging with EEA1-2xFYVE confirmed that the appearance of PI(3)P in membrane ruffles in MTMR6-depleted cells (Fig. 5*D* and Movie S6) but not in control cells (Movies S7 and S8) or INPP4B-depleted cells (Fig. S8 and Movies S9 and S10).

In summary, sequential conversion from PI(3,4,5)P_3 to PI in membrane ruffles during macropinocytosis is indicated: SHIP2, INPP4B, and MTMR6 catalyze the conversion of PI(3,4,5)P_3 to PI(3,4)P_2, PI(3,4)P_2 to PI(3)P, and PI(3)P to PI, respectively.

Inhibition of KCa3.1, a Ca^{2+}-Activated K^+ Channel, Impairs Macropinocytosis. We sought to identify molecules that function downstream of the 3-phosphorylated phosphoinositides generated during macropinocytosis. Because a patch clamping experiment indicated that KCa3.1 in the PM was activated by PI(3)P but not by other phosphoinositides (26), we focused on a Ca^{2+}-activated K^+ channel, KCa3.1.

To interfere with KCa3.1 function, we treated cells either with TRAM-34, a specific inhibitor of KCa3.1 (48, 49), or with siRNAs for KCa3.1. Pretreatment of cells with TRAM-34 for 5 min impaired the uptake of dextran (Fig. 6 *A* and *B*) but not the uptake of Tfn (Fig. S9 *A* and *B*). Similarly, knockdown of KCa3.1 impaired the uptake of dextran (Fig. 6 *A* and *B* and Fig. S9*C*) but not the uptake of Tfn (Fig. S9 *D* and *E*). Therefore, KCa3.1 shows the same specificity in endocytic pathways as MTMR6, MTMR9, and INPP4B and is essential for macropinocytosis. TRAM-34 treatment did not inhibit EGF-stimulated membrane ruffle formation (Fig. 6*C*) or actin polymerization (Fig. 6*D*). Knockdown of KCa3.1 did not also inhibit actin polymerization (Fig. S9*F*). Live imaging showed that the formation of macropinosomes, but not the formation of phase-dark ruffles and their movement, was severely impaired in cells treated with TRAM-34 (Fig. 6*E* and Movies S11 and S12).

We then examined the distribution of KCa3.1 in A431 cells. Before EGF stimulation, KCa3.1 tagged with GFP localized mostly at intracellular punctate structures, with little or no PM localization observed (Fig. 6*F*). Interestingly, KCa3.1 relocated to the PM, in particular, to membrane ruffles that were positive with F-actin after EGF stimulation. This result also supports the idea that KCa3.1 participates in macropinocytosis at membrane ruffles.

We exploited a mutant KCa3.1 (H358N) that is not activated by PI(3)P (50) to link KCa3.1 and the metabolism of phosphoinositides. Either WT or the mutant KCa3.1 tagged with GFP was expressed in cells to determine the effect on macropinocytosis. KCa3.1 (H358N) was targeted to membrane ruffles after EGF stimulation (Fig. S10) like WT KCa3.1; however, the mutant significantly suppressed the dextran uptake compared with the WT (Fig. 6*G*). Therefore, the mutant affected the step after the membrane ruffle formation during macropinocytosis. Given that KCa3.1 forms a tetramer (51) and that overexpression of H358N mutant acts in a dominant-negative fashion to suppress endogenous KCa3.1 function, activation of KCa3.1 by PI(3)P may be required for macropinocytosis. This result also suggests that INPP4B hydrolyzes PI(3,4)P_2 to produce PI(3)P, which activates KCa3.1 to complete macropinocytosis.

Knockdown of MTMR6, INPP4B, or SHIP2 did not affect the KCa3.1 relocation to membrane ruffles (Fig. 6*H*), indicating that

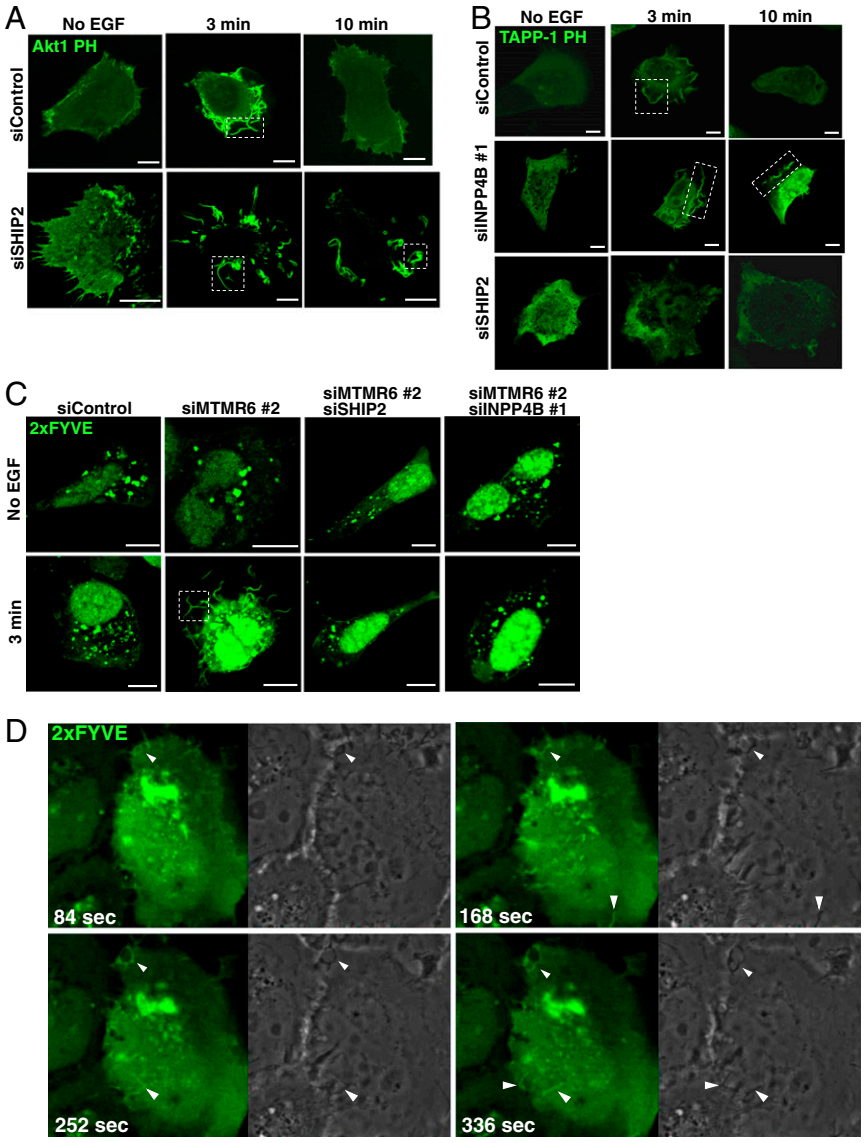

Fig. 5. Dynamics of PI(3,4,5)P_3, PI(3,4)P_2, and PI(3)P in membrane ruffles during macropinocytosis. (*A*) Cells were treated with the indicated siRNAs for 48 h, then transfected with Akt1-PH tagged with GFP, a specific probe for PI(3,4,5)P_3. After 24 h, cells were stimulated by EGF, then fixed at the indicated time points after EGF stimulation. Representative PI(3,4,5)P_3 at membrane ruffles is indicated by rectangles. (*B*) Cells were treated with the indicated siRNAs for 48 h, then transfected with TAPP1-PH tagged with GFP, a specific probe for PI(3,4)P_2. After 24 h, cells were stimulated by EGF, then fixed at the indicated time points after EGF stimulation. Representative PI(3,4)P_2 at membrane ruffles is indicated by a square. (*C*) Cells were treated with the indicated siRNAs for 48 h, then transfected with EEA1-2xFYVE tagged with GFP, a specific probe for PI(3)P. After 24 h, cells were stimulated by EGF, then fixed 3 min after EGF stimulation. Representative PI(3)P at membrane ruffles after EGF stimulation is indicated by rectangles. (Scale bars in *A*–*C*, 10 μm.) (*D*) Cells were treated with siRNA designed for MTMR6 for 48 h, then transfected with EEA1-2xFYVE tagged with GFP. Cells were stimulated by EGF, and live imaging was performed. Images of GFP (*Left*) and phase-contrast (*Right*) at the indicated time points are shown. Arrowheads indicate representative PI(3)P in membrane ruffles.

these phosphatases did not serve as a membrane scaffold for KCa3.1. Knockdown of KCa3.1 did not affect the MTMR6/MTMR9 relocation to membrane ruffles (Fig. S11), indicating that KCa3.1 did not serve as a membrane scaffold for MTMR6/MTMR9. Knockdown of KCa3.1 did not also affect the appearance of PI(3,4,5)P_3 and PI(3,4)P_2 (Fig. S7 *A* and *B*).

Discussion

Macropinocytosis was first described in macrophages more than eight decades ago (52). However, the lack of specific cargos and coat proteins has hampered precise biochemical and cell biological elucidation of this pathway. In this study, by making use of information of *C. elegans* mutants defective in fluid-phase endocytosis in coelomocytes (22, 23), we showed that mammalian 3-phosphatase MTMR6 and its cognate partner MTMR9 are required for macropinocytosis.

MTMR6 and MTMR9 were recruited to membrane ruffles during macropinocytosis, and the recruitment of MTMR6/MTMR9 to membrane ruffles is mediated by the PHG domains of MTMR6 and MTMR9. The PHG domain of MTMR6 binds to a number of phospholipids, with phosphatidic acid (PA) showing the highest affinity (41). Haga et al. (53) reported that PA produced by phospholipase D is required for macropinocytosis in COS-7 cells. Very recently, Bohdanowicz et al. (54) showed that the PA level of the plasma membrane is high in specialized phagocytic cells such as macrophages and dendritic cells, in which membrane ruffling and macropinocytosis are constitutively active. In this case, PA is supplied by the conversion of diacylglycerol (DG) to PA by DG kinase

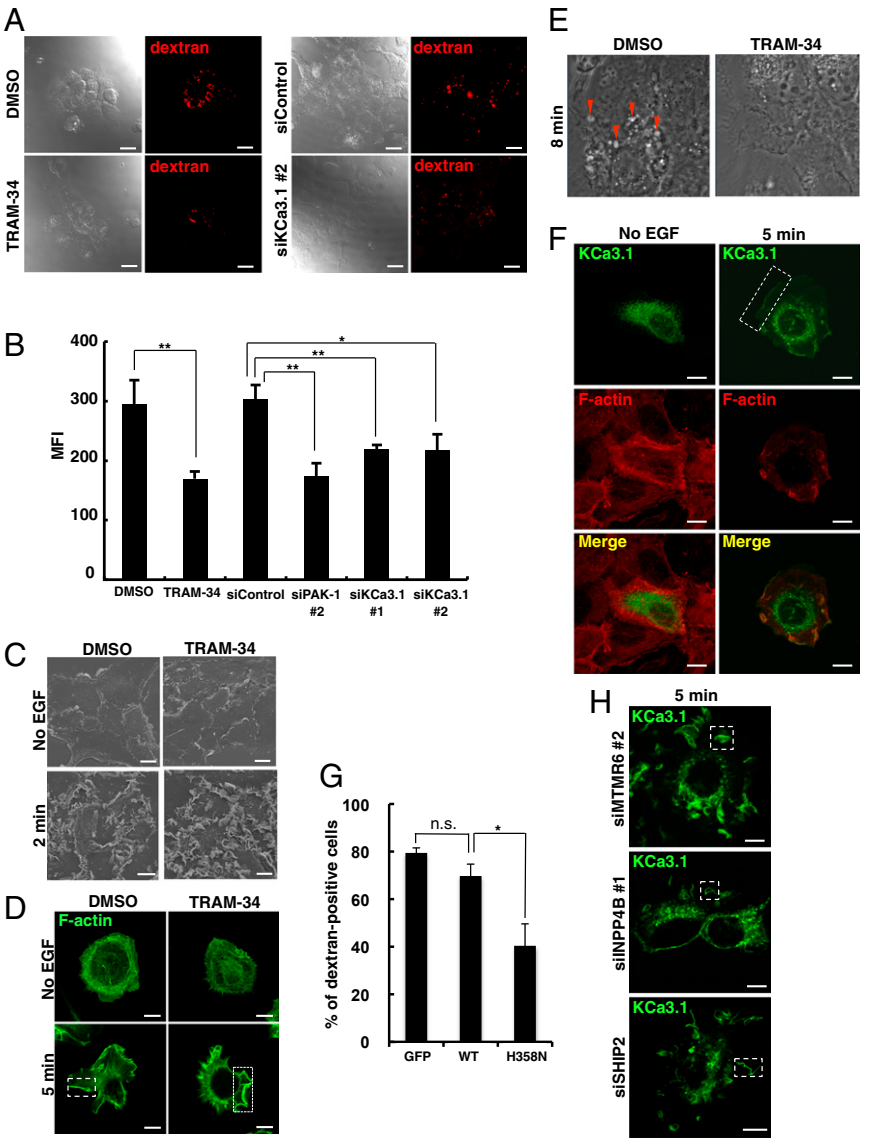

Fig. 6. KCa3.1 is essential for macropinocytosis. (*A*) Cells were pretreated with TRAM-34 (5 μM for 5 min) or treated with the indicated siRNAs. Cells were then stimulated by EGF for the uptake of TMR-dextran for 5 min. Brightfield and TMR-dextran fluorescence images are shown. (Scale bars, 20 μm.) (*B*) Cells processed as in *A* with fluorescein-dextran were subjected to FACS analysis. Data represent MFI ± SEM ($n = 3$). $^{*}P < 0.05$, $^{**}P < 0.01$. (*C*) Scanning electron micrographs of cells pretreated with TRAM-34 (5 μM for 5 min) with or without EGF stimulation. (Scale bars, 10 μm.) (*D*) F-actin staining by phalloidin in cells pretreated with TRAM-34 (5 μM for 5 min) with or without EGF stimulation. Representative F-actin–positive ruffles are indicated by rectangles. (Scale bars, 10 μm.) (*E*) Phase-contrast images 8 min after EGF stimulation of cells treated with TRAM-34 or vehicle alone. Representative macropinosomes (phase-bright objects) are indicated by red arrowheads. (*F*) Cells were transfected with GFP-KCa3.1. Cells were fixed 5 min after EGF stimulation, permeabilized, and stained for F-actin with phalloidin. Representative KCa3.1 at membrane ruffles after EGF stimulation is indicated by a square. (Scale bars, 10 μm.) (*G*) Cells were transfected with GFP, GFP-KCa3.1 (WT), or GFP-KCa3.1 (H358N). After 12 h, cells were starved for 3 h and stimulated with EGF for 5 min in the presence of TMR-dextran. Cells were then fixed and examined for the formation of dextran-positive macropinosomes. (*H*) Cells were treated with the indicated siRNAs for 48 h, then transfected with GFP-KCa3.1. After 24 h, cells were stimulated for 5 min with EGF, then fixed. Representative KCa3.1 at membrane ruffles after EGF stimulation is indicated by rectangles. (Scale bars, 10 μm.)

at the plasma membrane. It is thus tempting to hypothesize that PA generated with EGF stimulation recruits MTMR6/9 to the ruffles through the interaction of their PHG domains with PA.

We found that KCa3.1 is required for macropinocytosis. KCa3.1 is shown to be activated by PI(3)P by patch clamping (26). We observed that (*i*) PI(3)P was transiently generated and degraded in membrane ruffles, (*ii*) KCa3.1 was recruited from intracellular punctate structures to the membrane ruffles, and (*iii*) overexpression of a mutant KCa3.1 (H358N), which is not activated by PI(3)P, suppressed the uptake of dextran without affecting the membrane ruffle formation. All together, we assume that KCa3.1 is activated by PI(3)P produced in membrane ruffles to complete macropinocytosis. KCa3.1 effluxes intracellular K^+ upon activation, which leads to a Ca^{2+} influx (55). One possible function of KCa3.1 in macropinocytosis is that activated KCa3.1 induces Ca^{2+}-dependent events, such as cortical F-actin assembly and disassembly (56), to control the dynamics of membrane ruffles. KCa3.1 is also linked to cell volume (57). K^+ efflux through KCa3.1 decreases the intracellular solute concentration, which drives water efflux and causes the shrinkage of cell volume. We found that dextran uptake was enhanced by the supplementation of 0.0625 M sucrose to the medium (Fig. S12),

suggesting that water efflux induced by the additional sucrose facilitates macropinocytosis. We also found that the supplementation of 0.0625 M sucrose to cells treated with TRAM-34 restored the macropinocytic activity (Fig. S12), suggesting that KCa3.1 contributes to macropinocytosis, at least in part, by regulating local osmolarity through the decrease of the intracellular K^+ concentration.

Previous studies revealed that three phosphoinositides, PI(4,5)P_2, PI(3,4,5)P_3, and PI(3,4)P_2, transiently and sequentially emerge on membrane ruffles before macropinosome formation (18–20). The requirement of PI(3,4,5)P_3 in macropinocytosis is demonstrated using PI3K inhibitors (16). Phosphoinositide 5-phosphatase SHIP2, which converts PI(3,4,5)P_3 to PI(3,4)P_2, and a PI(3,4)P_2-binding protein, TAPP1 (tandem PH-domain-containing protein-1), are also required for macropinocytosis (17), indicating that PI(3,4)P_2 is not only a degradation product of PI(3,4,5)P_3 but has its own functions in macropinocytosis. In the present study we showed that INPP4B, which converts PI(3,4)P_2 to PI(3)P, and KCa3.1, which is specifically activated by PI(3)P, are required for macropinocytosis, indicating that PI(3)P is not only a degradation product of PI(3,4)P_2 but functions on its own in macropinocytosis. We also showed that knockdown of SHIP2, INPP4B, or MTMR6 abolished the production of the respective downstream phosphoinositides. Combined with the previous findings, we postulate that the sequential breakdown of PI(3,4,5)P_3 → PI(3,4)P_2 → PI(3)P → PI controls macropinocytosis through the specific effectors of the intermediate phosphoinositides, such as TAPP1 and KCa3.1, and that SHIP2, INPP4B, and MTMR6 catalyze the conversion of PI(3,4,5)P_3 to PI(3,4)P_2, PI(3,4)P_2 to PI(3)P, and PI(3)P to PI, respectively. In H-Ras G12V-expressing cells, PI(3,4,5)P_3 was detected on macropinosomes (58). In such cells, a partial degradation of PI(3,4,5)P_3 to produce PI(3,4)P_2, then to PI(3)P in membrane ruffles might be sufficient to complete macropinocytosis.

PI(3)P is constitutively expressed in early endosomes (47) and regulates membrane traffic through them (59). PI(3)P is also known to be generated in the PM. In adipocytes, PI(3)P is generated in the PM upon insulin stimulation and facilitates the translocation of the glucose transporter GLUT4 to the PM (60, 61). In HeLa cells, PI(3)P is generated in the PM in response to lysophosphatidic acid and stimulates cell migration (62). In both cases, PI(3)P lasted in the PM more than 10 min. In macropinocytosis, PI(3)P in the PM was detectable when PI(3)P phosphatase MTMR6 was knocked down and essential for macropinocytosis through downstream effectors, such as KCa3.1. Moreover, the rapid degradation of PI(3)P by MTMR6 is also essential for the completion of macropinocytosis. The lasting PI(3)P in cells depleted of MTMR6 may result in the constant activation of KCa3.1, which may lead to prolonged leakage of K^+ to the extracellular space and perturb the completion of macropinocytosis. Other PI(3)P effectors may exist, the inactivation of which is necessary for the process. Further study is needed to clarify the significance of PI(3)P degradation in macropinocytosis.

Macropinocytosis can be dissected into two morphologically distinct steps: one is the formation of membrane ruffles and the other is the closure of membrane ruffles. PAK-1, an effector that links RhoGTPases, such as Rac1 and Cdc42, to actin dynamics, regulates membrane ruffle formation during macropinocytosis (35–37). In the present study we found that a series of phosphoinositide phosphatases, which metabolize 3-phosphorylated phosphoinositide into PI, is required for macropinocytosis after the membrane ruffle formation. Thus, macropinocytosis can be dissected into two biochemically distinct steps: one is associated with actin polymerization, leading to membrane ruffle formation, and the other is associated with a sequential breakdown of 3-phosphorylated phosphoinositides, leading to the closure of membrane ruffles. The former step is shown to be inhibited by amiloride, an inhibitor of Na^+/H^+ exchange (5, 34). Because amiloride does not interfere with other endocytic pathways, amiloride has been extensively used as an indication of macropinocytosis. As shown in the present study, the latter step was inhibited by TRAM-34, an inhibitor of KCa3.1. Therefore, we postulate that macropinocytosis can also be dissected pharmacologically into two steps by amiloride and TRAM-34. Of note, it has recently been shown that 5-(*N*-ethyl-*N*-isopropyl)amiloride inhibits the growth of Ras-transformed tumor cells by impairment of macropinocytic activity of these cells (12). Specific inhibitors of KCa3.1, such as TRAM-34, may also be potential pharmacological drugs for cancer therapy.

The myotubularin family of constitutes a large group of conserved proteins, with 14 members in humans (MTM1, MTMR1–R13) (25). MTM1, MTMR2, and MTMR13 are causative genes for human genetic disorders such as X-linked centronuclear myopathy and Charcot–Marie–Tooth neuropathy (25). Myotubularins hydrolyze 3-phosphate from PI(3)P and PI(3,5)P_2 in vitro. Because PI(3)P and PI(3,5)P_2 are constitutively expressed in endosomes, myotubularins are demonstrated to function in the regulation of turnover of PI(3)P and PI(3,5)P_2 in endosomes. Some of the family members, including MTM1, MTMR2, and MTMR9, translocate from cytoplasm to the Rac1-induced membrane ruffles in the PM (63). In *Drosophila*, *myotubularin* (*mtm*), an ortholog of both MTM1 and MTMR2, is involved in the PM dynamics in hemocytes (64). We showed here that MTMR6 and MTMR9 translocate to membrane ruffles in the PM and are essential for its dynamics during macropinocytosis. Thus, some members of myotubularin family may function in the PM.

C. elegans has provided a powerful genetic system to decipher endocytic trafficking in a multicellular organism (23), such as degradation- and recycling pathways in the oocytes (65, 66) and phagocytosis of apoptosis cells by sheath cells (67, 68). These studies reveal that the trafficking pathways used in *C. elegans* are remarkably similar to those used in mammalian cells. Because the present results show that MTMR6 and MTMR9, which are mammalian orthologs of *mtm-6* and *mtm-9*, are essential for macropinocytosis, mammalian orthologs of other CUP genes might also function in macropinocytosis.

Materials and Methods

Reagents. The following reagents were purchased from the manufacturers as indicated: TMR-dextran (70,000 M_r), fluorescein-dextran (70,000 M_r), Lipofectamine 2000, Lipofectamine RNAiMAX, Alexa 488-phalloidin, Alexa 546-phalloidin, Alexa 488 donkey anti-rabbit IgG, and Alexa 594 donkey anti-mouse IgG (Invitrogen); EGF, amiloride, TRAM-34, human holo-Tfn, and mouse anti-myc antibody (9E10) (Sigma); rabbit anti-myc antibody (Upstate); mouse anti-calnexin antibody (BD Transduction); and 4% (wt/vol) glutaraldehyde (Nakalai). Tfn-Alexa 488 was prepared with the aid of Alexa 488 carboxylic acid succinimidyl ester (Invitrogen).

Cell Culture. A431 cells were maintained in DMEM supplemented with 10% (vol/vol) FCS and 100 U/mL penicillin, 100 μg/mL streptomycin, and 0.29 mg/mL glutamine.

General Methods and Strains of *C. elegans*. Worm cultures, genetic crosses, and other *C. elegans* methods were performed according to standard protocols (69). The following mutations and transgenes were used: *mtm-6 (ok330)III*, *mtm-9(ar479)V*, *cdIs54[pcc-1::MANS::GFP, myo-2::GFP]*, and *arIs37[myo-3p::ssGFP]*. All mutant alleles in this study were obtained from *Caenorhabditis* Genetic Center (University of Minnesota, Minneapolis). All mutations were backcrossed five times before further analysis. Worms were mounted on a 5% (wt/vol) agar pad on a glass slide and immobilized in 20 mM azide. Micrographs were taken on a Zeiss Axio Imager M1 microscope.

Ex Vivo Fluid-Phase Endocytosis Assay of Coelomocytes. In vitro culture of coelomocytes was performed as previously described (30). The isolated coelomocytes were incubated in 150 μL medium (Gibco, #18045-088) containing TMR-dextran (100 μg/mL, 70,000 M_r) in a glass-bottom dish (Iwaki) for 20 min at 20 °C. After washing three times with medium, fluorescence images were acquired by confocal microscopy (LSM 510 META; Zeiss).

Plasmids. Mouse MTMR6 and MTMR9 were amplified with cDNA derived from mouse brain using the following pairs of primers: 5′-CGTCGCGAATTCATGGAGCACATCCGGACAAC-3′ (sense primer) and 5′-GGATCACGGCGGCCGCCTAACAAGTCATTCTGGCCA-3′ (antisense primer); 5′-GCTGCGGAATTCATGGAGTTTGCGGAGCTGAT-3′ (sense primer) and 5′-TCTTTCAAGCGGCCGCTCATAGCCCATCCTCTGTTT-3′ (antisense primer). These products were introduced into pcDNA3 with myc-tag (Invitrogen). MTMR6 CR/AA was generated with the following pair of primers: 5′-CATCGGAGGCGTGGACCAACACACT-3′ (sense primer) and 5′-GGTGGGACGCCACCTCCCAAGTGTG-3′ (antisense primer). Mouse MTMR6 (WT and CR/AA) were subcloned into pEGFP-C2 (Clontech). MTMR6 PHG was generated with full-length MTMR6 using the following pair of primers and introduced into pEGFP-C2: 5′-GCGTCGCTCGAGCATGGAGCACATCCGGACAAC-3′ (sense primer) and 5′-ATAAGAGAATTCCTAGAGATCTTCATATTTTGCTT-3′ (antisense primer). MTMR9 PHG was generated with full-length MTMR9 using the following pair of primers and introduced into pEGFP-C2: 5′-GCTGCGCTCGAGATGGAGTTTGCGGAGCTGAT-3′ (sense primer) and 5′-AGGGTAGAATTCTCAGACCGAGTCCAGAGTGGACA-3′ (antisense primer). MTMR6 ΔPHG was generated with full-length MTMR6 using the following pair of primers and introduced into pcDNA3 with myc-tag: 5′- TATGAAGAATTCTATGCCTTCTCTTATAATCC-3′ (sense primer) and 5′-GGATCACGGCGGCCGCCTAACAAGTCATTCTGGCCA-3′ (antisense primer). MTMR9 ΔPHG was generated with full-length MTMR9 using the following pair of primers and introduced into pcDNA3 with myc-tag: 5′- CTGGACGAATTCACCCTGATGTACCCTTTCTT-3′ (sense primer) and 5′- TCTTTCAAGCGGCCGCTCATAGCCCATCCTCTGTTT-3′ (antisense primer). pCAGGS-GFP vectors with 2xFYVE (EEA1), PH (TAPP1), and PH (Akt) were kind gifts from T. Sasaki (Akita University, Akita, Japan). Human KCa3.1 and KCa3.1 (H358N) with pEGFP-C2 were previously described (50).

siRNAs. The following validated siRNA duplex oligomers (Invitrogen) were used for knockdown experiments: CGGACGACCAAGGUCGAACAAGUAA (MTMR6 siRNA #1), GGAUAGCAAGCAAACCAAUAAUUGU (MTMR6 siRNA #2), GGGACUACAAGAUUUGUGAAACUUA (MTMR6 siRNA #3), GGAUCACUGGGUACCAUCAUCAUAA (MTMR9 siRNA #1), CCUGGAAUGGAGGAAUGCUUGAAUA (MTMR9 siRNA #2), GCCAGUUCCAUUGAGGCAUUGUCUA (MTMR9 siRNA #3), GGAAUGGAUGGCUCUGUCAAGCUAA (PAK-1 siRNA #2), GCUACUCCAUAGAUUUGAAACAGAA (INPP4B siRNA #1), CCAGACAGCUUGAAGAAUUCUUUAA (INPP4B siRNA #2), CAGAAUGUUUGAGUCACUACCUCUA (INPP4B siRNA #3), GAGGUUGGAGUUACCUCCCAGUUCA (SHIP2 siRNA), CGCCAUCGGUUCGUGGCCAAGCUUU (KCa3.1 siRNA #1), and GAAGCCUGGAUGUUCUACAAACAUA (KCa3.1 siRNA #2). Control siRNA was from Nippon EGT.

Transfection. Transfections of plasmids were performed using Lipofectamine 2000 (Invitrogen) according to the manufacturer's instructions. Unless otherwise specified, subsequent experiments were performed 24 h after transfection. Transfections of siRNAs (40 nM) were performed using RNAiMAX reagent (Invitrogen) according to the manufacturer's instructions. Unless otherwise specified, subsequent experiments were performed 72 h after transfection.

RT-PCR. Total RNA was extracted from cells using Isogen II (Nippongene) and reverse-transcribed using the High Capacity cDNA Reverse Transcription kit (Applied Biosystems). Quantitative real-time PCR was performed using SYBR Green PCR Master Mix (TaKaRa) and Light-Cycler 480 (Roche Diagnostics). GAPDH was used as a reference gene. The following primers were used: human PAK-1 forward (CTCCACCAGATGCTTTGACC) and reverse (TCGCCCACACTCACTATGCT); human MTMR6 forward (CGACTCTCATCAAAAAGAAACCTG) and reverse (AAGGGGGCATCCAGAAGTAG); human MTMR9 forward (TGTGGCTCCTCCATTCAAAC) and reverse (TTCAAGCATTCCTCCATTCC); human INPP4B forward (TGAACCGAGCCAAGCAGTC) and reverse (CCACAAACCAATCCAGCAAG); human KCa3.1 forward (GCAGGAACTGGCATTGGAC) and reverse (CACGATGAGGCAGAGGAGTAA); GAPDH forward (GCCAAGGTCATCCATGACAACT) and reverse (GAGGGGCCATCCACAGTCTT).

Macropinocytosis Assay. A431 cells were serum-starved in DMEM for 3 h at 37 °C. Cells were then incubated with 0.25 mg/mL TMR- or fluorescein-dextran and 100 ng/mL EGF in DMEM for 5 min at 37 °C. For imaging, cells were fixed with 4% (wt/vol) formaldehyde in PBS at room temperature for 20 min. For quantitative analysis with FACS, cells were detached from the dish with 0.25% (wt/vol) trypsin-EDTA for 5 min at 37 °C, collected, spun briefly, and resuspended in 0.6 mL of ice-cold PBS. Cells were sorted using FACSCalibur with CellQuest software (BD Biosciences). When necessary, cells were incubated with 1 mM amiloride for 30 min at 37 °C before EGF stimulation.

Tfn Uptake. A431 cells were serum-starved in DMEM for 30 min at 37 °C. Cells were then incubated with 50 μg/mL of Tfn-Alexa 488 in DMEM for 5 min at 37 °C. Cells were then chilled on ice and acid-washed to remove Tfn-Alexa 488 on the PM. For imaging, cells were fixed with 4% (wt/vol) formaldehyde in PBS at room temperature for 20 min. For quantitative analysis, FACS was used as described.

Immunofluorescence Microscopy. Cells were fixed with 4% (wt/vol) formaldehyde in PBS at room temperature for 15 min and permeabilized with 0.1% (wt/vol) Triton X-100 in PBS at room temperature for 10 min. Blocking was carried out with 3% (wt/vol) BSA in PBS for 30 min. Cells were incubated with primary antibodies at room temperature for 2 h. After washing with PBS, cells were incubated with secondary antibodies at room temperature for 1 h, washed with PBS, then mounted. Fluorescence images were acquired by confocal microscopy (LSM 510 META; Zeiss).

Live Cell Imaging. Transfected A431 cells were washed once using prewarmed Ringer's buffer (RB) [10 mM Hepes·NaOH (pH 7.2), 155 mM NaCl, 5 mM KCl, 2 mM $CaCl_2$, 1 mM $MgCl_2$, 2 mM NaH_2PO_4, 10 mM D-glucose, and 0.5 mg/mL BSA] and assembled in a RB-filled Attofluor cell chamber (Molecular Probes) on the thermo-controlled stage (Tokai Hit). Live cell imaging was performed using Axio observer Z1 inverted microscope equipped with laser scanning unit (LSM700; Zeiss) and Plan-Apochromat 63×/N.A. 1.4 lens under ZEN2009 software (Zeiss). Time-lapse images of GFP fluorescence and brightfield phase-contrast were acquired for every 15 s using 1.0% laser power of 10 mW 488-nm laser and assembled to QuickTime movie files.

Scanning Electron Microscopy. A431 cells were cultured on coverslips were serum-starved for 3 h. After EGF stimulation, cells were fixed with 4% (wt/vol) glutaraldehyde in 0.1 M phosphate buffer, pH 7.4, for 1 h at 4 °C. The specimens were postfixed with 1% (wt/vol) OsO_4, stained with 1% (wt/vol) tannic acid and 1% (wt/vol) OsO_4, and processed for scanning electron microscopy as previously described (16). The specimens were dried using a CO_2 critical-point dryer (Hitachi HCP), coated with an osmium plasma coater (OPC40; Nippon Laser & Electronics), and observed by a field-emission scanning electron microscope (Hitachi S900) at 6 kV.

ACKNOWLEDGMENTS. We thank Mr. Shoken Lee, Mr. Tatsuyuki Matsudaira, and Mr. Kojiro Mukai (University of Tokyo) for technical assistance, Dr. Kenji Kontani (University of Tokyo) for help with ex vivo fluid-phase endocytosis assay using coelomocytes, and Dr. Kiyotaka Hatsuzawa (Tottori University Faculty of Medicine) and Dr. Jenna E. McKenzie (State of California Department of Pesticide Regulation) for comments on the manuscript. This work was supported by the Program for Promotion of Basic and Applied Researches for Innovations in Bio-oriented Industry (H.A.), the Core Research for Evolutional Science and Technology, Japan Science and Technology Agency (H.A.), grants-in-aid from the Japanese Ministry of Education, Culture, Sports, Science, and Technology (20370045 to H.A., 23390039 and 24659087 to N.A., and 80534510 to K.K.), and National Institutes of Health Grant R01AI080583 (to E.Y.S.).

1. Conner SD, Schmid SL (2003) Regulated portals of entry into the cell. *Nature* 422 (6927):37–44.
2. Swanson JA (2008) Shaping cups into phagosomes and macropinosomes. *Nat Rev Mol Cell Biol* 9(8):639–649.
3. Lim JP, Gleeson PA (2011) Macropinocytosis: an endocytic pathway for internalising large gulps. *Immunol Cell Biol* 89(8):836–843.
4. Haigler HT, McKanna JA, Cohen S (1979) Rapid stimulation of pinocytosis in human carcinoma cells A-431 by epidermal growth factor. *J Cell Biol* 83(1):82–90.
5. West MA, Bretscher MS, Watts C (1989) Distinct endocytotic pathways in epidermal growth factor-stimulated human carcinoma A431 cells. *J Cell Biol* 109(6 Pt 1):2731–2739.
6. Bar-Sagi D, Feramisco JR (1986) Induction of membrane ruffling and fluid-phase pinocytosis in quiescent fibroblasts by ras proteins. *Science* 233(4768):1061–1068.
7. Hoffmann PR, et al. (2001) Phosphatidylserine (PS) induces PS receptor-mediated macropinocytosis and promotes clearance of apoptotic cells. *J Cell Biol* 155(4):649–659.
8. Meier O, et al. (2002) Adenovirus triggers macropinocytosis and endosomal leakage together with its clathrin-mediated uptake. *J Cell Biol* 158(6):1119–1131.
9. Garrett WS, et al. (2000) Developmental control of endocytosis in dendritic cells by Cdc42. *Cell* 102(3):325–334.
10. West MA, et al. (2004) Enhanced dendritic cell antigen capture via toll-like receptor-induced actin remodeling. *Science* 305(5687):1153–1157.
11. Mercer J, Helenius A (2009) Virus entry by macropinocytosis. *Nat Cell Biol* 11(5): 510–520.
12. Commisso C, et al. (2013) Macropinocytosis of protein is an amino acid supply route in Ras-transformed cells. *Nature* 497(7451):633–637.

13. Vanhaesebroeck B, et al. (2001) Synthesis and function of 3-phosphorylated inositol lipids. *Annu Rev Biochem* 70:535–602.
14. Fruman DA, Meyers RE, Cantley LC (1998) Phosphoinositide kinases. *Annu Rev Biochem* 67:481–507.
15. Di Paolo G, De Camilli P (2006) Phosphoinositides in cell regulation and membrane dynamics. *Nature* 443(7112):651–657.
16. Araki N, Johnson MT, Swanson JA (1996) A role for phosphoinositide 3-kinase in the completion of macropinocytosis and phagocytosis by macrophages. *J Cell Biol* 135(5):1249–1260.
17. Hasegawa J, et al. (2011) SH3YL1 regulates dorsal ruffle formation by a novel phosphoinositide-binding domain. *J Cell Biol* 193(5):901–916.
18. Araki N, Egami Y, Watanabe Y, Hatae T (2007) Phosphoinositide metabolism during membrane ruffling and macropinosome formation in EGF-stimulated A431 cells. *Exp Cell Res* 313(7):1496–1507.
19. Yoshida S, Hoppe AD, Araki N, Swanson JA (2009) Sequential signaling in plasma-membrane domains during macropinosome formation in macrophages. *J Cell Sci* 122(Pt 18):3250–3261.
20. Welliver TP, Swanson JA (2012) A growth factor signaling cascade confined to circular ruffles in macrophages. *Biol Open* 1(8):754–760.
21. Welliver TP, Chang SL, Linderman JJ, Swanson JA (2011) Ruffles limit diffusion in the plasma membrane during macropinosome formation. *J Cell Sci* 124(Pt 23):4106–4114.
22. Fares H, Greenwald I (2001) Genetic analysis of endocytosis in *Caenorhabditis elegans*: coelomocyte uptake defective mutants. *Genetics* 159(1):133–145.
23. Fares H, Grant B (2002) Deciphering endocytosis in *Caenorhabditis elegans*. *Traffic* 3(1):11–19.
24. Robinson FL, Dixon JE (2006) Myotubularin phosphatases: policing 3-phosphoinositides. *Trends Cell Biol* 16(8):403–412.
25. Hnia K, Vaccari I, Bolino A, Laporte J (2012) Myotubularin phosphoinositide phosphatases: cellular functions and disease pathophysiology. *Trends Mol Med* 18(6): 317–327.
26. Srivastava S, et al. (2005) The phosphatidylinositol 3-phosphate phosphatase myotubularin- related protein 6 (MTMR6) is a negative regulator of the Ca2+-activated K+ channel KCa3.1. *Mol Cell Biol* 25(9):3630–3638.
27. Srivastava S, et al. (2006) Phosphatidylinositol 3-phosphate indirectly activates KCa3.1 via 14 amino acids in the carboxy terminus of KCa3.1. *Mol Biol Cell* 17(1):146–154.
28. Srivastava S, et al. (2006) Phosphatidylinositol-3 phosphatase myotubularin-related protein 6 negatively regulates CD4 T cells. *Mol Cell Biol* 26(15):5595–5602.
29. Dang H, Li Z, Skolnik EY, Fares H (2004) Disease-related myotubularins function in endocytic traffic in *Caenorhabditis elegans*. *Mol Biol Cell* 15(1):189–196.
30. Nakae I, et al. (2010) The arf-like GTPase Arl8 mediates delivery of endocytosed macromolecules to lysosomes in *Caenorhabditis elegans*. *Mol Biol Cell* 21(14):2434–2442.
31. Bednarek EM, Schaheen L, Gaubatz J, Jorgensen EM, Fares H (2007) The plasma membrane calcium ATPase MCA-3 is required for clathrin-mediated endocytosis in scavenger cells of *Caenorhabditis elegans*. *Traffic* 8(5):543–553.
32. Zou J, Chang SC, Marjanovic J, Majerus PW (2009) MTMR9 increases MTMR6 enzyme activity, stability, and role in apoptosis. *J Biol Chem* 284(4):2064–2071.
33. Hamasaki M, Araki N, Hatae T (2004) Association of early endosomal autoantigen 1 with macropinocytosis in EGF-stimulated A431 cells. *Anat Rec A Discov Mol Cell Evol Biol* 277(2):298–306.
34. Koivusalo M, et al. (2010) Amiloride inhibits macropinocytosis by lowering submembranous pH and preventing Rac1 and Cdc42 signaling. *J Cell Biol* 188(4):547–563.
35. Dharmawardhane S, et al. (2000) Regulation of macropinocytosis by p21-activated kinase-1. *Mol Biol Cell* 11(10):3341–3352.
36. Liberali P, et al. (2008) The closure of Pak1-dependent macropinosomes requires the phosphorylation of CtBP1/BARS. *EMBO J* 27(7):970–981.
37. Mercer J, Helenius A (2008) Vaccinia virus uses macropinocytosis and apoptotic mimicry to enter host cells. *Science* 320(5875):531–535.
38. Motley A, Bright NA, Seaman MN, Robinson MS (2003) Clathrin-mediated endocytosis in AP-2-depleted cells. *J Cell Biol* 162(5):909–918.
39. Schaletzky J, et al. (2003) Phosphatidylinositol-5-phosphate activation and conserved substrate specificity of the myotubularin phosphatidylinositol 3-phosphatases. *Curr Biol* 13(6):504–509.
40. Naughtin MJ, et al. (2010) The myotubularin phosphatase MTMR4 regulates sorting from early endosomes. *J Cell Sci* 123(Pt 18):3071–3083.
41. Choudhury P, et al. (2006) Specificity of the myotubularin family of phosphatidylinositol-3-phosphatase is determined by the PH/GRAM domain. *J Biol Chem* 281(42): 31762–31769.
42. Norris FA, Atkins RC, Majerus PW (1997) The cDNA cloning and characterization of inositol polyphosphate 4-phosphatase type II. Evidence for conserved alternative splicing in the 4-phosphatase family. *J Biol Chem* 272(38):23859–23864.
43. Ivetac I, et al. (2005) The type Ialpha inositol polyphosphate 4-phosphatase generates and terminates phosphoinositide 3-kinase signals on endosomes and the plasma membrane. *Mol Biol Cell* 16(5):2218–2233.
44. Gewinner C, et al. (2009) Evidence that inositol polyphosphate 4-phosphatase type II is a tumor suppressor that inhibits PI3K signaling. *Cancer Cell* 16(2):115–125.
45. Thomas CC, Deak M, Alessi DR, van Aalten DM (2002) High-resolution structure of the pleckstrin homology domain of protein kinase b/akt bound to phosphatidylinositol (3,4,5)-trisphosphate. *Curr Biol* 12(14):1256–1262.
46. Dowler S, et al. (2000) Identification of pleckstrin-homology-domain-containing proteins with novel phosphoinositide-binding specificities. *Biochem J* 351(Pt 1):19–31.
47. Gillooly DJ, et al. (2000) Localization of phosphatidylinositol 3-phosphate in yeast and mammalian cells. *EMBO J* 19(17):4577–4588.
48. Wulff H, et al. (2000) Design of a potent and selective inhibitor of the intermediate-conductance Ca2+-activated K+ channel, IKCa1: a potential immunosuppressant. *Proc Natl Acad Sci USA* 97(14):8151–8156.
49. Bradding P, Wulff H (2009) The K+ channels K(Ca)3.1 and K(v)1.3 as novel targets for asthma therapy. *Br J Pharmacol* 157(8):1330–1339.
50. Srivastava S, et al. (2006) Histidine phosphorylation of the potassium channel KCa3.1 by nucleoside diphosphate kinase B is required for activation of KCa3.1 and CD4 T cells. *Mol Cell* 24(5):665–675.
51. Garneau L, Klein H, Parent L, Sauvé R (2010) Toward the rational design of constitutively active KCa3.1 mutant channels. *Methods Enzymol* 485:437–457.
52. Lewis WH (1931) Pinocytosis. *Bull Johns Hopkins Hosp* 49:17–27.
53. Haga Y, Miwa N, Jahangeer S, Okada T, Nakamura S (2009) CtBP1/BARS is an activator of phospholipase D1 necessary for agonist-induced macropinocytosis. *EMBO J* 28(9): 1197–1207.
54. Bohdanowicz M, et al. (2013) Phosphatidic acid is required for the constitutive ruffling and macropinocytosis of phagocytes. *Mol Biol Cell* 24(11):1700–1712, S1–S7.
55. Feske S, Skolnik EY, Prakriya M (2012) Ion channels and transporters in lymphocyte function and immunity. *Nat Rev Immunol* 12(7):532–547.
56. Janmey PA (1994) Phosphoinositides and calcium as regulators of cellular actin assembly and disassembly. *Annu Rev Physiol* 56:169–191.
57. Schwab A, Nechyporuk-Zloy V, Fabian A, Stock C (2007) Cells move when ions and water flow. *Pflugers Arch* 453(4):421–432.
58. Porat-Shliom N, Kloog Y, Donaldson JG (2008) A unique platform for H-Ras signaling involving clathrin-independent endocytosis. *Mol Biol Cell* 19(3):765–775.
59. Simonsen A, et al. (1998) EEA1 links PI(3)K function to Rab5 regulation of endosome fusion. *Nature* 394(6692):494–498.
60. Falasca M, Maffucci T (2012) Regulation and cellular functions of class II phosphoinositide 3-kinases. *Biochem J* 443(3):587–601.
61. Maffucci T, Brancaccio A, Piccolo E, Stein RC, Falasca M (2003) Insulin induces phosphatidylinositol-3-phosphate formation through TC10 activation. *EMBO J* 22(16): 4178–4189.
62. Maffucci T, et al. (2005) Class II phosphoinositide 3-kinase defines a novel signaling pathway in cell migration. *J Cell Biol* 169(5):789–799.
63. Laporte J, et al. (2002) Functional redundancy in the myotubularin family. *Biochem Biophys Res Commun* 291(2):305–312.
64. Velichkova M, et al. (2010) *Drosophila* Mtm and class II PI3K coregulate a PI(3)P pool with cortical and endolysosomal functions. *J Cell Biol* 190(3):407–425.
65. Grant B, Hirsh D (1999) Receptor-mediated endocytosis in the *Caenorhabditis elegans* oocyte. *Mol Biol Cell* 10(12):4311–4326.
66. Balklava Z, Pant S, Fares H, Grant BD (2007) Genome-wide analysis identifies a general requirement for polarity proteins in endocytic traffic. *Nat Cell Biol* 9(9):1066–1073.
67. Kinchen JM, et al. (2008) A pathway for phagosome maturation during engulfment of apoptotic cells. *Nat Cell Biol* 10(5):556–566.
68. Kinchen JM (2010) A model to die for: signaling to apoptotic cell removal in worm, fly and mouse. *Apoptosis* 15(9):998–1006.
69. Brenner S (1974) The genetics of *Caenorhabditis elegans*. *Genetics* 77(1):71–94.